THE JOURNAL OF IMMUNOLOGY

Endothelial Induction of fgl2 Contributes to Thrombosis during Acute Vascular Xenograft Rejection

Anand Ghanekar, Michael Mendicino, Hao Liu, Wei He, Mingfeng Liu, Robert Zhong, M. James Phillips, Gary A. Levy and David R. Grant

J Immunol 2004;172;5693-5701

The Journal of Immunology is published twice each month by
The American Association of Immunologists, Inc.,
9650 Rockville Pike, Bethesda, MD 20814-3994.

Print ISSN: 0022-1767 Online ISSN: 1550-6606.

Endothelial Induction of fgl2 Contributes to Thrombosis during Acute Vascular Xenograft Rejection[1]

Anand Ghanekar,[2]*†‡ Michael Mendicino,[2]*§ Hao Liu,*† Wei He,* Mingfeng Liu,*† Robert Zhong,‖ M. James Phillips,¶ Gary A. Levy,*†§ and David R. Grant[3]*‡

Thrombosis is a prominent feature of acute vascular rejection (AVR), the current barrier to survival of pig-to-primate xenografts. Fibrinogen-like protein 2 (fgl2/fibroleukin) is an inducible prothrombinase that plays an important role in the pathogenesis of fibrin deposition during viral hepatitis and cytokine-induced fetal loss. We hypothesized that induction of fgl2 on the vascular endothelium of xenografts contributes to thrombosis associated with AVR. We first examined fgl2 as a source of procoagulant activity in the pig-to-primate combination. The porcine fgl2 (pfgl2) was cloned and its chromosomal locus was identified. Recombinant pfgl2 protein expressed in vitro was detected on the cell surface and generated thrombin from human prothrombin. Studies of pig-to-baboon kidney xenografts undergoing AVR in vivo revealed induction of pfgl2 expression on graft vascular endothelial cells (ECs). Cultured porcine ECs activated by human TNF-α in vitro demonstrated induction of pfgl2 expression and enhanced activation of human prothrombin. The availability of gene-targeted fgl2-deficient mice allowed the contribution of fgl2 to the pathogenesis of AVR to be directly examined in vivo. Hearts heterotopically transplanted from *fgl2*$^{+/+}$ and *fgl2*$^{+/-}$ mice into Lewis rats developed AVR with intravascular thrombosis associated with induction of *fgl2* in graft vascular ECs. In contrast, xenografts from *fgl2*$^{-/-}$ mice were devoid of thrombosis. These observations collectively suggest that induction of fgl2 on the vascular endothelium plays a role in the pathogenesis of AVR-associated thrombosis. Manipulation of fgl2, in combination with other interventions, may yield novel strategies by which to overcome AVR and extend xenograft survival. ***The Journal of Immunology,*** **2004, 172: 5693–5701.**

Thrombosis is a characteristic but incompletely understood element of inflammation, innate immune responses, and acquired immune disorders (1–5). Localized induction of procoagulant molecules on the vascular endothelium is thought to play an important role in this process. Distinct from tissue factor, a major initiator of the extrinsic coagulation cascade, novel procoagulants have been identified that can independently contribute to fibrin deposition. Fibrinogen-like protein 2 (fgl2 or fibroleukin),[4] one of several proteins with a highly conserved fibrinogen-related domain, is a direct prothrombinase that generates thrombin from prothrombin in the absence of a classical prothrombinase complex (6). We have recently demonstrated that induction of fgl2 expression on the surface of hepatic reticuloendothelial cells accounts for fibrin deposition in human and murine models of fulminant viral hepatitis; inhibition of fgl2, through the use of neutralizing Abs or *fgl2* knockout mice, prevents fibrin deposition, liver necrosis, and death (7, 8). Inhibition of fgl2 has also been shown to prevent abortion in a murine model through prevention of cytokine-triggered intravascular thrombosis at the uteroplacental interface (9).

Fibrin deposition is a prominent feature of acute vascular xenograft rejection (AVR; also referred to as delayed xenograft rejection or acute humoral xenograft rejection), the major barrier currently preventing long-term survival of pig-to-primate solid organ xenografts (10). Xenotransplantation of tissues between species has emerged as a potential solution to the shortage of human organs for transplantation, with pigs having been identified as the most promising source of organs (11). Hyperacute rejection (HAR) of porcine organs by primates, initiated by binding of preformed xenoantibodies to the galactosyl-α1,3-galactose (α-gal) epitope, has been overcome through the development of transgenic pigs that express human complement regulatory proteins such as human decay-accelerating factor (hDAF) (12).

Despite intensive immune suppression and depletion of xenoantibodies, survival of transgenic pig-to-primate solid organ xenografts has been limited to weeks by AVR. AVR is also observed in concordant rodent models of xenotransplantation, in which HAR is naturally averted due to the absence of high-titer preformed xenoantibodies (13). In addition to microangiopathy and tissue infiltration by small numbers of macrophages and NK cells, intravascular fibrin deposition and thrombosis are hallmarks of AVR (10).

The pathophysiology of fibrin deposition during AVR has not been clearly defined. It has been proposed that activation of vascular endothelial cells (ECs) in the graft contributes to the development of a prothrombotic microenvironment. This hypothesis is supported by studies that demonstrate that exposure of ECs to

*Multi-Organ Transplant Program, †Institute of Medical Science, and Departments of ‡Surgery, §Immunology, and ¶Laboratory Medicine and Pathobiology, University of Toronto, Toronto, Ontario, Canada; and ‖Multi-Organ Transplant Program, University of Western Ontario, London, Ontario, Canada

Received for publication December 17, 2003. Accepted for publication February 20, 2004.

The costs of publication of this article were defrayed in part by the payment of page charges. This article must therefore be hereby marked *advertisement* in accordance with 18 U.S.C. Section 1734 solely to indicate this fact.

[1] This work was supported by grants from the Heart and Stroke Foundation of Canada and the Canadian Institutes of Health Research.

[2] A.G. and M.M. contributed equally to this study.

[3] Address correspondence and reprint requests to Dr. David R. Grant, Multi-Organ Transplant Program, Toronto General Hospital, 585 University Avenue, NCSB-11C-1248, Toronto, Ontario, Canada, M5G 2N2. E-mail address: david.grant@uhn.on.ca

[4] Abbreviations used in this paper: fgl2, fibrinogen-like protein 2; AVR, acute vascular rejection; HAR, hyperacute rejection; α-gal, galactosyl-α1,3-galactose; hDAF, human decay-accelerating factor; EC, endothelial cell; pfgl2, porcine fgl2; PAEC, porcine aortic endothelial cell; mfgl2, mouse fgl2; RPA, RNase protection assay; FISH, fluorescence in situ hybridization; DAPI, 4′,6′-diamidino-2-phenylindole; His, polyhistidine; H5, High Five; BS-IB$_4$, *Bandeiraea simplicifolia* isolectin B$_4$; MSB, Martius scarlet blue; POD, postoperative day; UTR, untranslated region.

0022-1767/04/$02.00

xenoantibodies, complement, platelets, immune cells, and cytokines results in loss of natural anticoagulant pathways and acquisition of a procoagulant phenotype through a combination of morphological changes and altered gene expression (14, 15). In the pig-to-primate combination, thrombosis may also be favored by disordered thromboregulation resulting from identified incompatibilities between human and porcine coagulation factors (16).

The generation of thrombin, in particular, within the microvasculature has important physiological consequences. In addition to generating fibrin from fibrinogen, thrombin activates platelets and exerts direct effects on vascular smooth muscle cells and ECs, serving as a potent inflammatory mediator (17). Studies suggest that dysregulated thrombin generation may play an important role in mediating xenograft AVR, in that inhibition of thrombin in vivo has been associated with prolonged xenograft survival (18). In vitro studies have demonstrated not only that human thrombin is able to activate porcine ECs (19), but that porcine ECs directly generate thrombin from human prothrombin in the absence of other coagulation factors (20, 21). The mechanism by which the latter occurs has not been identified.

We hypothesized that induction of fgl2 expression on the vascular endothelium of xenografts contributes to the fibrin deposition associated with AVR. To investigate this hypothesis, we cloned the porcine fgl2 (pfgl2), assessed its functional relevance across species barriers, and studied its expression both in vivo in pig-to-primate kidney xenografts and in vitro in cultured porcine aortic endothelial cells (PAECs). We subsequently used gene-targeted *fgl2* knockout mice in a rodent model of AVR to directly examine the contribution of fgl2 in vivo to the pathogenesis of AVR-associated xenograft thrombosis.

Materials and Methods

PCR, RT-PCR, and DNA manipulations

PCR was performed using an Advantage 2 PCR kit (Clontech, Palo Alto, CA). RT-PCR was performed using a one-step RT-PCR kit (Qiagen, Valencia, CA). The pCR 2.1 TOPO and pCR II TOPO TA cloning kits (Invitrogen, Carlsbad, CA) were used for subcloning of PCR products. Restriction enzymes and DNA ligase for conventional subcloning (22) were purchased from Invitrogen. Gel extractions were performed using a QIAquick Gel Extraction kit (Qiagen). Plasmid DNA was amplified using a QIAprep Spin Miniprep kit or a HiSpeed Plasmid Midi kit (Qiagen). Oligonucleotide primer synthesis and DNA sequencing were performed at The Centre for Applied Genomics at the Hospital for Sick Children (Toronto, Ontario, Canada). Samples were sequenced on both strands by automated fluorescent dye-terminator cycle sequencing based on the dideoxynucleotide method.

Preparation of cDNA probes

Mouse *fgl2* (*mfgl2*) cDNA sequences were amplified by PCR from a plasmid containing the full-length *mfgl2* coding region (6) using sense 5′-TAGGAAGGAGAAGCAGTGGG-3′ and antisense 5′-GCTTGAAATTCTTGGGCCTA-3′ for a 659-bp portion of exon 2 and sense 5′-ATGCAAAGGACCAGATCCAG-3′ with antisense 5′-GTGTTCTTGGCTGGGACACT-3′ for a 161-bp portion of exon 1. Porcine cDNA sequences were amplified by RT-PCR from RNA isolated from PAECs (see below). A 1341-bp porcine *fgl2* probe was amplified using sense 5′-GCCACCGCAGAGATGAAG-3′ and antisense 5′-TTATGGCTTAAAGTACTTGGGTCTG-3′. A 700-bp E-selectin probe was amplified using sense 5′-CAGTGCTTATTGCCAGCAGA-3′ and antisense 5′-GGTGAAGTGGCAGGTTGACT-3′. A 64-bp probe for 18S rRNA (loading control) was generated by PCR from pTRI RNA 18S plasmid DNA (Ambion, Austin, TX) using sense 5′-AATTCCAGCTCCAATAGCGTA-3′ and antisense 5′-CCAAGATCCAACTACGAGCTTT-3′. The cDNA sequences were labeled with [α-^{32}P]dCTP using the RediPrime DNA labeling system (Amersham Biosciences, Piscataway, NJ). Unincorporated radionucleotides were removed using ProbeQuant G-50 microcolumns (Amersham Biosciences). Radioactivity was measured using a Beckman LS 5000 TD liquid scintillation counter (Beckman Instruments, Fullerton, CA).

Genomic cloning

A radioactively labeled cDNA probe corresponding to the second exon of *mfgl2* was used for hybridization screening of a bacteriophage EMBL3 SP6/T7 adult porcine genomic library (Clontech) according to the manufacturer's protocol. DNA from plaque-purified clones was isolated from high-titer plate lysates using a Lambda Midi Kit (Qiagen). Relevant regions of the DNA inserts of purified library clones were sequenced after mapping by restriction enzyme analysis and localization of *fgl2* by Southern blotting of restriction fragments with *mfgl2* cDNA probes. Additional genomic DNA sequence at the 3′ end of the porcine *fgl2* gene was obtained by PCR using genomic DNA extracted from porcine tissues (obtained from a local slaughterhouse) using a DNEasy Mini kit (Qiagen). PCR was performed using a sense primer (5′-AATAGGATACCAAATGTAAAT-3′) derived from porcine genomic library clone sequences and an antisense primer (5′-TGGTGTTCCTCTATTTGCCTCT-3′) derived from human *fgl2* sequence (GenBank) to generate a 1.1-kb product that shared ~700 bp of sequence with library clones and contained ~400 bp of novel sequence.

Northern blotting

Total RNA was extracted from porcine tissues (obtained from a local slaughterhouse) using TRIzol reagent (Invitrogen) or from cultured cells using an RNEasy Mini kit (Qiagen). Twenty micrograms of total RNA for each sample was resolved by electrophoresis in 1.2% agarose-formaldehyde gels in MOPS-EDTA-sodium acetate buffer (Sigma-Aldrich, St. Louis, MO), transferred to Hybond-N$^+$ membranes (Amersham Biosciences) by capillary action in 20× SSC, and UV cross-linked. Membranes were prehybridized for 1 h and then hybridized with labeled probes for 2 h at 68°C in 5 ml of ExpressHyb hybridization solution (Clontech), after which washing, autoradiography, and stripping were conducted per the manufacturer's instructions.

RACE

A SMARTRACE cDNA amplification kit was used with touchdown thermal cycling protocols (Clontech). One microgram of porcine small intestinal total RNA was used as a template for synthesis of first-strand cDNA for both 5′ and 3′ RACE. For 5′ RACE, the gene-specific antisense primers were 5′-CGCCATGTTCTGGTGAAGTTGGTGCT-3′ and 5′-CCCCCATGGTCTCCATGTCACAGTAA-3′ (nested). For 3′ RACE, the gene-specific sense primers were 5′-AAGCTGAAGCTGTCGAACTGGTGCTG-3′ and 5′-CCAAGGAAGAGATCGACGGGCTTCAG-3′ (nested). PCR products were subcloned and sequenced.

RNase protection assays (RPAs)

Three RPA probe sequences were amplified from porcine genomic DNA by PCR, subcloned into the dual promoter Sp6/T7 pCR II TOPO (Invitrogen), and sequenced. A 1120-bp probe for the 5′ end of the predicted *fgl2* mRNA was amplified with 5′-AACAAAGTCTACTGCAAGAGG-3′ and 5′-CGTTAGGTTTGCCACCTTGT-3′. A 2602-bp probe for the predicted 3′ end of the short *fgl2* mRNA variant was amplified with 5′-TGATGGAAGCACCAACTTCA-3′ and 5′-GGAGTGCACTTTTGATCACAGAAA-3′. A 1233-bp probe for the predicted 3′ end of the longer *fgl2* mRNA was amplified with 5′-AATAGGATACCAAATGTAAATG-3′ and 5′-TGGTGTTCCTCTATTTGCCTCT-3′. A DIG RNA labeling kit (Roche, Indianapolis, IN) was used to synthesize digoxigenin-labeled sense or antisense probes by in vitro transcription from linearized recombinant plasmids. For each RPA reaction, 600 pg of antisense or sense (negative control) probe was coprecipitated with 100 μg of porcine small intestinal total RNA using ethanol precipitation (22). Hybridization and RNase digestion were performed using an RNase protection kit (Roche). RPA products were resolved using 6% Tris borate EDTA/urea PAGE (Invitrogen) and electroblotted onto positively charged nylon membranes (Roche). Chemiluminescent detection was performed with a DIG luminescent detection kit (Roche) followed by autoradiography.

Fluorescence in situ hybridization (FISH)

Lymphocytes were isolated from heparinized whole pig blood (a kind gift from C. Feindel, University Health Network, Toronto, Ontario, Canada) by density gradient centrifugation and were cultured in α-MEM supplemented with 15% FBS, 1% L-glutamine, and PHA at 37°C for 72 h. Cells were harvested and slide mounted using standard procedures including hypotonic treatment, fixation, and air drying. The 12.8-kb genomic DNA insert of a *pfgl2*-containing bacteriophage clone was excised with *Sal*I, gel purified, and biotinylated with dATP using a BioNick labeling kit (Invitrogen) for use as a probe. The FISH procedure was performed as described (23, 24). FISH signals and the 4′,6′-diamidino-2-phenylindole (DAPI)

banding pattern were photographed separately. Alignment of FISH mapping data with chromosomal bands was achieved by superimposing FISH signals with DAPI banded chromosomes (25).

Generation of rabbit polyclonal Abs against pfgl2

A C-terminal peptide from pfgl2 (YRSSFKEAKMMIRPKYFKP) was synthesized and conjugated to keyhole limpet hemocyanin (Dalton Chemical Laboratories, Toronto, Ontario, Canada). After collection of preimmune serum, New Zealand White rabbits were immunized with 200 μg of peptide in CFA. Fourteen days after immunization, boosting and bleeding cycles were initiated in which rabbits were boosted with 100 μg of peptide in IFA and then bled 1 wk thereafter for collection of serum. IgG was purified from serum on a Poly-Prep chromatography column (Bio-Rad, Hercules, CA) using Protein G Sepharose 4 Fast-Flow (Amersham Biosciences) according to the manufacturer's protocol. IgG samples were analyzed by SDS-PAGE and Coomassie blue staining, and concentrations were determined using a bicinchoninic acid protein assay reagent kit (Pierce, Rockford, IL).

Baculovirus expression of recombinant pfgl2 protein

The full-length coding region of porcine *fgl2* was amplified from porcine small intestinal RNA by RT-PCR (sense 5′-GCCACCGCAGAGAT GAAG-3′, antisense 5′-TTATGGCTTAAAGTACTTGGGTCTG-3′) and ligated into the pAcHLT-C baculovirus transfer vector (BD PharMingen, San Diego, CA) to create pAcHLT-C/*pfgl2*. Cotransfection of *Spodoptera frugiperda* 9 cells (BD PharMingen) with linearized BaculoGold baculovirus DNA (BD PharMingen) and pAcHLT-C/*pfgl2* generated a recombinant baculovirus encoding pfgl2 protein with a polyhistidine (His) tag. High Five (H5) cells (Invitrogen), used for high-yield protein production, were infected with baculovirus at a multiplicity of infection of 5, harvested 72 h after infection, and subjected to analysis by Western blotting, flow cytometry, or functional assay as described below. *S. frugiperda* 9 and H5 cells were maintained according to the manufacturers' instructions. Amplification and titering of viral stocks, plaque purification, and viral DNA isolation and sequencing were performed as described (44). Wild-type Ac-NPV baculovirus (BD PharMingen) was used as a control.

PAEC culture

Porcine aortic segments (obtained from a local slaughterhouse) were instilled with 0.075% collagenase (Type IV-S; Sigma-Aldrich) in Dulbecco's PBS (Invitrogen) and incubated for 10 min at 37°C. Contents were removed into DMEM (Invitrogen) and centrifuged at 500 $\times$ *g* for 10 min at room temperature. Cells were plated in complete medium consisting of DMEM supplemented with 10% FBS (Invitrogen), penicillin (100 U/ml)/streptomycin (100 μg/ml) (Invitrogen), heparin (10 U/ml; Sigma-Aldrich), and endothelial mitogen (100 μg/ml; Biomedical Technologies, Stoughton, MA). Cells were propagated as monolayers at 37°C with 5% CO_2 and were used for experiments until passage four. For experiments, PAECs were maintained at confluence for 24–48 h, after which complete growth medium was replaced with complete medium alone or complete medium containing 20 ng/ml human TNF-α (Sigma-Aldrich), 100 μg/ml α-gal-binding *Bandeiraea simplicifolia* isolectin B_4 ($BS\text{-}IB_4$) (Sigma-Aldrich), or 50% human serum or combinations thereof. Human serum was pooled from healthy volunteers and was used both with and without inactivation of complement by heating at 56°C for 30 min. Cells harvested at various time points were subjected to analysis by Northern blot, Western blot, and functional assay as described.

Western blotting

Samples were resolved using SDS-PAGE under reducing or nonreducing conditions and were transferred to Protran nitrocellulose membranes (Schleicher & Schuell, Keene, NH) using standard methods (22). Membranes were blocked with 5% nonfat dry milk in PBS containing 0.05% Tween 20. Primary and secondary Abs were diluted in blocking solution and sequentially incubated with membranes for 60 min at room temperature, separated by five washes of 5 min each in PBS containing 0.05% Tween 20. Chemiluminescent detection was performed using ECL (Amersham Biosciences) followed by autoradiography. Data presented are representative of three separate experiments.

For H5 cells, whole cell lysates from 10^5 cells were analyzed under reducing conditions. The primary Abs were monoclonal mouse anti-HisG or an IgG2a isotype control (1/5000 dilution; Invitrogen), and the secondary Ab was rabbit anti-mouse Ig HRP (1/5000; Amersham Biosciences). For PAECs, samples were harvested in lysis buffer (50 mM Tris-HCl (pH 7.5), 150 mM NaCl, 1% Triton X-100, 0.1% SDS, 1% sodium deoxycholate), sheared by passage through a 25-gauge needle, and then cleared by centrifugation. Seventy micrograms of protein, determined using a bicinchoninic acid protein assay reagent kit (Pierce), was loaded per lane under reducing or nonreducing conditions. The primary Abs were polyclonal rabbit anti-pfgl2 IgG (10 μg/ml), preimmune rabbit IgG (10 μg/ml, negative control), or rabbit anti-β-actin (1/3000, loading control; Sigma-Aldrich), and the secondary Ab was goat anti-rabbit Ig HRP (1/2500; BD PharMingen).

Flow cytometry

Uninfected, pfgl2 baculovirus-infected, and wild-type baculovirus-infected H5 cells were harvested, counted, and washed three times with PBS. Aliquots of 10^6 cells were blocked with 10% goat serum (Sigma-Aldrich) in PBS containing 1% BSA (BSA/PBS) for 30 min before sequential 60-min incubations with primary and secondary Abs diluted in BSA/PBS. All steps were performed on ice, protected from light, and separated by two washes with cold BSA/PBS. Primary Abs were mouse anti-HisG or an IgG2a isotype control (both 1/5000; Invitrogen), and the secondary Ab was goat anti-mouse IgG FITC (1/5000; Santa Cruz Biotechnology, Santa Cruz, CA). Analysis was performed using a Beckman-Coulter flow cytometer. Data presented are representative of three separate experiments.

Thrombin generation assays

H5 cells or PAECs were harvested, counted, and washed three times with cold reaction buffer (20 mM HEPES, 150 mM sodium chloride, and 5 mM calcium chloride (pH 7.4)). Cells were resuspended in reaction buffer at a concentration of 3×10^7 cells/ml. A total of 3×10^5 cells (10 μl) were mixed with an equal volume of human prothrombin (Enzyme Research Laboratories, South Bend, IN) in reaction buffer to give a final prothrombin concentration of 10 μM for H5 cells or 1 μM for PAECs. For additional negative controls, cells were incubated with reaction buffer alone (no prothrombin), and prothrombin was incubated with reaction buffer alone (no cells). Reactions were incubated for 30 min at 37°C and were run in triplicate for each experiment. To measure thrombin generation, 125 μl of cold assay buffer (50 mM Tris, 227 mM sodium chloride, 1% BSA, and 1% sodium azide (pH 8.3)) was added to each reaction. After centrifugation at 14,000 rpm for 5 min to pellet cells, 145 μl of supernatant from each reaction mixture supernatant was transferred to one well of a flat-bottom 96-well plate. Fifteen microliters of Chromozym TH (Roche), a chromogenic substrate of human thrombin, was added to each well and the plate was incubated at room temperature. OD_{405} was measured at regular intervals using an automated plate reader (Titertek, Huntsville, AL) to generate a plot of the change in OD_{405} per minute. The thrombin activity of each experimental sample was calculated by comparison with the absorbance curve generated by known concentrations of human thrombin (Sigma-Aldrich) at time points within the linear range of the chromogenic reaction. Means and SDs for each experimental condition were calculated from combined data generated from separate experiments. Statistically significant differences ($p < 0.05$) were identified by one-way ANOVA for independent samples (for H5 cells) or one-way ANOVA with repeated measures (for PAECs); Tukey's test was used for post hoc analysis.

Histopathology and immunohistochemistry of porcine tissues

Formalin-fixed, paraffin-embedded necropsy tissues from previously reported hDAF pig-to-baboon kidney xenotransplantation experiments were studied (26, 27). Nontransplanted hDAF pig kidneys were studied as negative controls. Five-micrometer, slide-mounted sections were stained with H&E using standard methods. For immunohistochemistry, a Vectastain Elite ABC kit (Vector Laboratories, Burlingame, CA) was used in combination with rabbit anti-pfgl2 IgG or preimmune rabbit IgG primary Abs. After dewaxing and hydration, sections were pretreated with 0.5% pepsin (Sigma-Aldrich) in 1N hydrochloric acid for 30 min at 37°C. Endogenous peroxidase activity was blocked by incubating slides in 0.3% hydrogen peroxide in methanol for 30 min at room temperature. Additional blocking was performed with normal goat serum as well as with an avidin/biotin blocking kit (Vector Laboratories). Sections were incubated with primary Abs (5 μg/ml in 0.1% BSA/PBS) at 4°C overnight in a humidified chamber. Incubations with biotinylated goat anti-rabbit IgG and the avidin/biotin complex were performed according to the kit protocol. Chromogenic detection of peroxidase activity was conducted with diaminobenzidine tetrahydrochloride (Sigma-Aldrich). Sections were counterstained, dehydrated, and mounted according to conventional methods.

Mouse-to-rat cardiac xenotransplantation

The production of mice with a targeted disruption of the *fgl2* gene has been described previously (8). The targeting construct used to generate these mice contains a β-galactosidase reporter gene under the transcriptional

control of the native *fgl2* promoter, allowing the use of β-galactosidase staining to localize *fgl2* transcriptional activation in vivo in $fgl2^{+/-}$ or $fgl2^{-/-}$ mice. Male littermates used for all experiments were derived from the third generation of $fgl2^{+/-}$ mice backcrossed to the C57BL/6 background. Inbred adult male Lewis rats were obtained from Charles River Breeding Laboratories (Montreal, Quebec, Canada). Animals were handled in accordance with guidelines set by the Canadian Council on Animal Care.

Animals were anesthetized with an i.p. injection of Somnotol (MTC Pharmaceuticals, Cambridge, Ontario, Canada) at a dose of 65 mg/kg. Each donor mouse heart was removed as previously described (28) and was implanted heterotopically in the groin of a Lewis rat. The ascending aorta and pulmonary artery of the donor heart were anastomosed to the recipient femoral artery and femoral vein, respectively. Grafts were observed for 30 min after reperfusion and subsequently were assessed daily by palpation. Cessation of graft function was inferred by an absence of palpable ventricular contractions and confirmed by direct visual examination of the graft. No immune suppression was administered in these experiments. Data presented are representative of 10 experiments for each mouse genotype.

Histopathology and β-galactosidase staining of murine tissues

For light microscopy, formalin-fixed, paraffin-embedded specimens were sectioned and stained with H&E or Martius scarlet blue (MSB) according to standard procedures. β-Galactosidase staining was performed on 6-μm cryostat sections of tissue snap frozen with liquid nitrogen in OCT compound (Sakura Finetek, Torrance, CA). A β-galactosidase staining kit (Invitrogen) was used with technical modifications required for use of the protocol with tissue sections. $Fgl2^{+/+}$ cardiac xenografts were used as negative controls.

Results

Molecular cloning and chromosomal localization of pfgl2

Mapping and sequencing of porcine genomic library clones in combination with genomic PCR yielded sequence data corresponding to the full-length porcine *fgl2* gene. To identify a source of RNA from which the porcine *fgl2* cDNA could be cloned, total RNA samples from a variety of porcine tissues were studied. As shown in Fig. 1*a*, Northern analysis revealed that two *fgl2* mRNA transcripts of 4.3 kb and 1.5 kb were constitutively present in different amounts in all tissues studied. Sequence analysis of overlapping 5′ and 3′ RACE products (Fig. 1*b*) identified the porcine *fgl2* mRNA transcription initiation site, 3′ cleavage/polyadenylation sites, and coding region as well as exon-intron junctions in the genomic sequence. Although 3′ RACE was able to identify a consensus cleavage and polyadenylation signal (AATAAA) for the 1.5-kb mRNA species, RPAs were required to demonstrate the second predicted 3′ cleavage/polyadenylation signal corresponding to the longer mRNA transcript of 4.3 kb (Fig. 1*c*). RPA also confirmed the findings of 5′ RACE (data not shown). Fig. 1*d* schematically illustrates the composite structures of the porcine *fgl2* gene and mRNA transcripts identified by our cloning strategy.

The longest open reading frame, shared by both mRNA species, encodes a 442-aa protein that shares 89% overall sequence similarity with human fgl2 and 77% with mouse fgl2. The C-terminal fibrinogen-related domain, which shares strong sequence similarity with the β and γ chains of fibrinogen, is highly conserved in pfgl2, as is the serine protease clan SE motif SXXK (at position 93) that has been shown by site-directed mutagenesis to account for the coagulation activity of murine fgl2 (6). As shown in Fig. 2, FISH identified *fgl2* as a single-copy gene in the porcine genome, localized to chromosome 9q16-17. All porcine *fgl2* sequence data have been annotated and deposited in GenBank under accession number AY112657.

Recombinant pfgl2 protein is expressed on the cell surface and generates active thrombin from human prothrombin

A baculovirus expression system was used to express recombinant His-tagged porcine fgl2 protein. As shown in Fig. 3*a*, Western blotting with an anti-His Ab demonstrated a single band of ~55 kDa in lysates from H5 cells that were infected with pfgl2-encoding baculovirus. As shown in Fig. 3*b*, flow cytometry analysis of H5 cells stained with an anti-His Ab revealed that recombinant pfgl2 protein was expressed on the cell surface. Staining with an IgG2a isotype control Ab was negative in both Western and flow cytometry analyses. Fig. 3*c* illustrates the results of a chromogenic assay for the generation of active thrombin from human prothrombin, in which intact H5 cells expressing pfgl2 protein on their surface were found to generate significantly more thrombin than do uninfected cells or cells infected with wild-type baculovirus. Negative control reactions processed in parallel, lacking either prothrombin or cells, did not generate any thrombin activity.

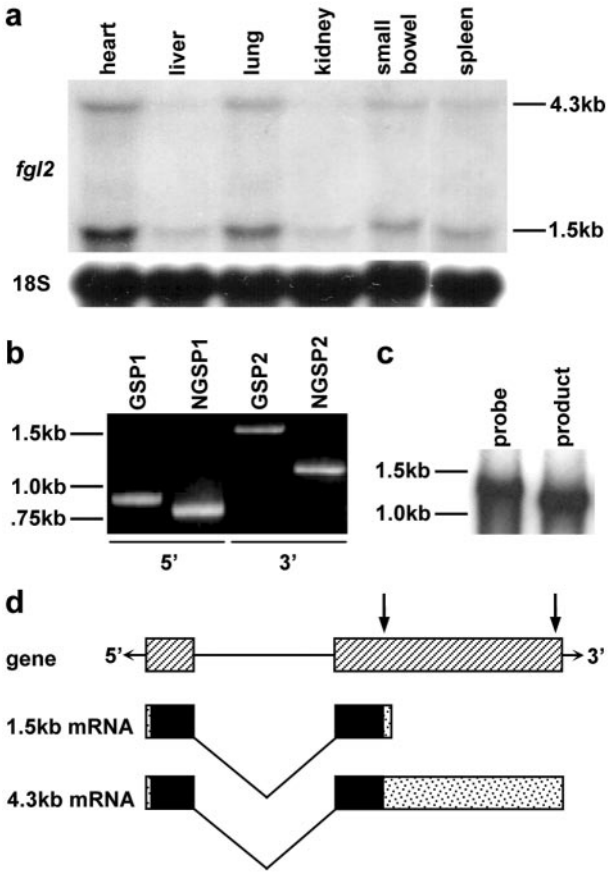

FIGURE 1. Identification of the *pfgl2* cDNA. *a*, Northern blot probed with an *mfgl2* exon 2 cDNA probe demonstrating two *fgl2* mRNA transcripts of 4.3 kb and 1.5 kb in porcine tissues. *b*, Ethidium bromide-stained agarose gel demonstrating overlapping 5′ and 3′ RACE PCR products generated by gene-specific primers (GSP1, GSP2) and nested gene-specific primers (NGSP1, NGSP2) that correspond to the 1.5-kb porcine *fgl2* transcript. *c*, Antidigoxigenin immunoblot demonstrating the shortened RPA product of an antisense probe containing the predicted 3′ cleavage/polyadenylation site of the 4.3-kb porcine *fgl2* transcript. *d*, Schematic illustration of the *pfgl2* gene and mRNA transcripts. Hatched boxes represent exons, arrows represent 3′ cleavage/polyadenylation (poly(A)) signals, filled boxes represent coding regions, and dotted boxes represent UTRs. Two poly(A) signals in the second exon result in two mRNA transcripts that share the same 5′ UTR and coding region, but differ with respect to their 3′ UTRs.

Porcine fgl2 is induced in pig-to-baboon xenografts undergoing AVR in vivo

Pig-to-baboon kidney xenografts were analyzed for expression of pfgl2 in vivo. Examination of untransplanted hDAF pig kidneys revealed normal histology (data not shown). Examination of all

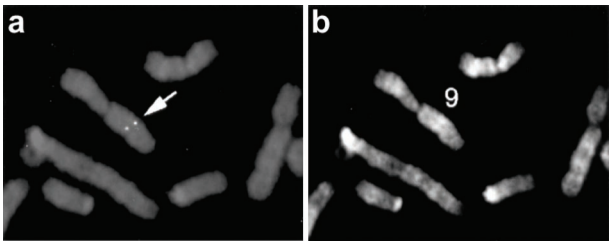

FIGURE 2. FISH localization of the *pfgl2* chromosomal locus. *a*, Fluorescent signal of the *pfgl2* genomic probe hybridized to a single locus on porcine metaphase chromosomes (arrow). *b*, DAPI staining and banding pattern analysis revealed the locus identified in *a* to be chromosome 9q16-17.

xenograft specimens revealed features of AVR, as previously reported (26, 27). Vascular features of AVR included thrombotic microangiopathy, interstitial hemorrhage, fibrinoid medial necrosis of small to medium-sized arteries and arterioles, intravascular thrombosis, and fibrin deposition. Glomerular manifestations of AVR included thrombotic microangiopathy, glomerular capillary microaneurysms, increased mesangial cells or mesangiolysis, and glomerular necrosis. Parenchymal features of AVR included interstitial edema and scant infiltration by macrophages or polymorphonuclear cells. Renal tubules demonstrated focal vacuolization, epithelial cell degenerative changes, or necrosis.

As illustrated in Fig. 4, immunostaining for fgl2 was observed in the vessels and glomeruli of xenografts that showed features of AVR. Staining of fgl2 appeared to localize primarily to arterioles and small to medium-sized arteries that displayed features of AVR such as fibrinoid necrosis, luminal narrowing, and fibrin deposition. Fgl2 staining was observed in the walls of these vessels and predominantly involved the endothelium. Glomeruli of xenografts with more advanced AVR demonstrated diffuse, dense staining for fgl2, whereas glomeruli of grafts with milder rejection demonstrated staining that appeared to localize specifically to capillary endothelial cells. Immunostaining for fgl2 in untransplanted hDAF pig kidneys and immunostaining of xenograft tissues with preimmune IgG were both negative (data not shown).

Cultured porcine endothelial cells activated by human TNF-α demonstrate induction of pfgl2 expression and enhanced activation of human prothrombin

Primary cultures of PAECs were studied for expression of pfgl2 in vitro. Northern analysis of total RNA extracted from PAECs demonstrated minimal constitutive *pfgl2* mRNA levels, which increased in response to incubation with 20 ng/ml human TNF-α, as shown in Fig. 5*a*. Activation of PAECs by TNF-α was confirmed by the observation of increased E-selectin mRNA levels, as described by other investigators (29). Fig. 5*a* also demonstrates that, although PAECs were activated by the engagement of α-gal by BS-IB_4, as demonstrated by increased E-selectin mRNA levels, *fgl2* mRNA levels did not increase. Human serum (with or without heat inactivation of complement) had no effect on *pfgl2* mRNA levels in PAECs as measured by Northern analysis (data not shown).

Incubation of PAECs with human TNF-α (20 ng/ml) also resulted in induction of pfgl2 protein expression, which was detected in the cell lysate by Western blot (Fig. 5*b*). Pfgl2 was minimally expressed in PAECs at baseline, but steadily increased up to 24 h after exposure of cells to TNF-α. The molecular mass of pfgl2 was shown to be 65 kDa.

Intact PAECs, harvested at various time points after activation with TNF-α, were analyzed for their ability to generate thrombin

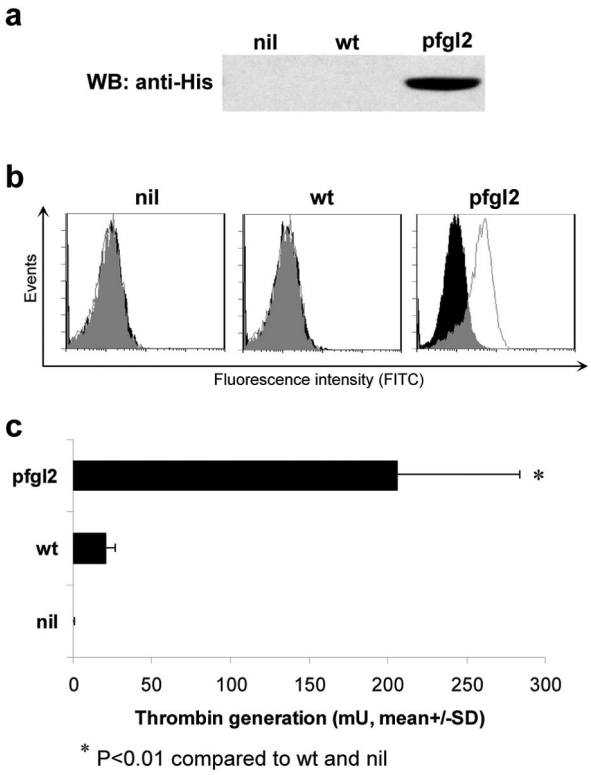

FIGURE 3. Cell surface expression and generation of active thrombin from human prothrombin by recombinant pfgl2 protein. *a*, Representative Western blot with an anti-His Ab demonstrating the ~55-kDa recombinant pfgl2 protein expressed by H5 cells infected with pfgl2-encoding baculovirus, in comparison with uninfected cells (nil) or cells infected with wild-type baculovirus (wt). *b*, Representative flow cytometry analysis of H5 cells with an anti-His Ab (open histogram) or isotype control Ab (filled histogram) demonstrating surface expression of recombinant pfgl2 protein on cells infected with pfgl2-encoding baculovirus, in comparison with nil or wt (overlapping regions appear gray). *c*, Graph demonstrating significantly greater generation of thrombin from human prothrombin by H5 cells expressing recombinant pfgl2 protein in comparison with nil or wt ($p < 0.01$; graph represents combined data from three separate experiments).

from human prothrombin. As shown in Fig. 5*c*, thrombin generation by PAECs was evident at baseline but increased in parallel with fgl2 protein expression. Negative control reactions processed in parallel, lacking either prothrombin or cells, did not generate any thrombin activity, confirming that the assay was not contaminated by thrombin before the reaction with exogenously added prothrombin (data not shown).

AVR of mouse-to-rat xenografts is associated with endothelial induction of fgl2 and is prevented by the use of fgl2-deficient organs

Mouse-to-rat cardiac xenografts from $fgl2^{+/+}$ and $fgl2^{+/-}$ donor mice developed typical features of AVR as described above, including interstitial hemorrhage and intravascular thrombosis, beginning on postoperative day 1 (POD 1), with cessation of graft function by POD 3 (Fig. 6, *a* and *b*). In contrast, xenografts from $fgl2^{-/-}$ donors were devoid of intravascular fibrin deposition and thrombosis throughout the postoperative period (Fig. 6, *c* and *d*). In the absence of recipient immune suppression, xenografts from $fgl2^{-/-}$ donors demonstrated progressive infiltration by recipient leukocytes and were rejected by POD 3 (Fig. 6, *c* and *d*).

Xenografts from $fgl2^{+/-}$ and $fgl2^{-/-}$ mice were studied by β-galactosidase staining to localize transcriptional induction of

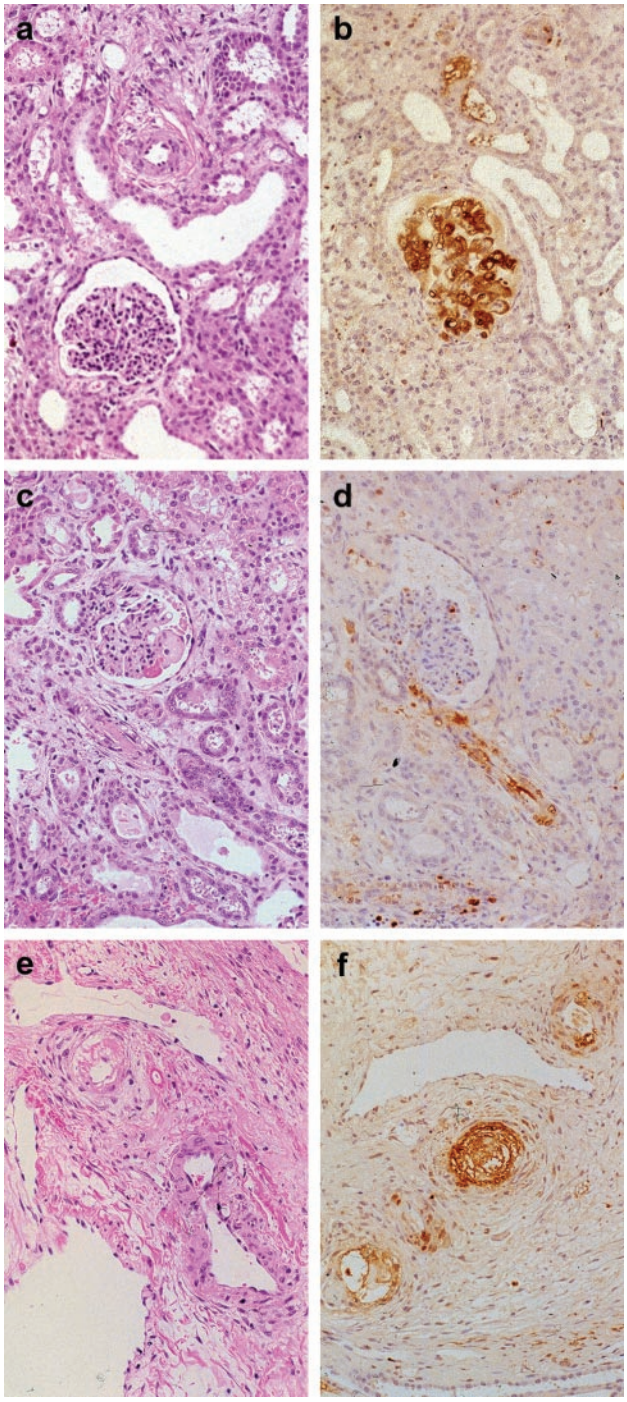

FIGURE 4. H&E staining (*a*, *c*, and *e*) and immunoperoxidase staining for pfgl2 protein (*b*, *d*, and *f*) in pig-to-baboon kidney xenografts (pfgl2 stains brown). *a*, Representative area of renal cortex showing mild vascular changes with thickening of the walls of small arteries, perivascular edema, and separation of the outer media and adventitia; glomerulus demonstrates microangiopathic changes, increased cellularity, bloodless appearance, and increased mesangial cells typical of AVR. *b*, Representative glomerular tuft with changes typical of AVR, staining positively for fgl2. This appearance was found in ~30% of glomeruli in the sections examined. *c*, Section of renal cortex showing changes similar to those described in *a*, in addition to focal mesangiolysis, hemorrhage, and fibrin deposition in the glomerulus. An arteriole in the vicinity of the glomerulus has a lumen that was partially occluded by fibrin. *d*, An arteriole in the vicinity of the glomerulus, similar to that described in *c*, demonstrates staining for fgl2 with positivity in the vessel wall predominantly involving endothelial cells. This finding was consistent in almost all small to medium-sized arteries in all sections (the glomerulus shows only minimal involvement in this section).

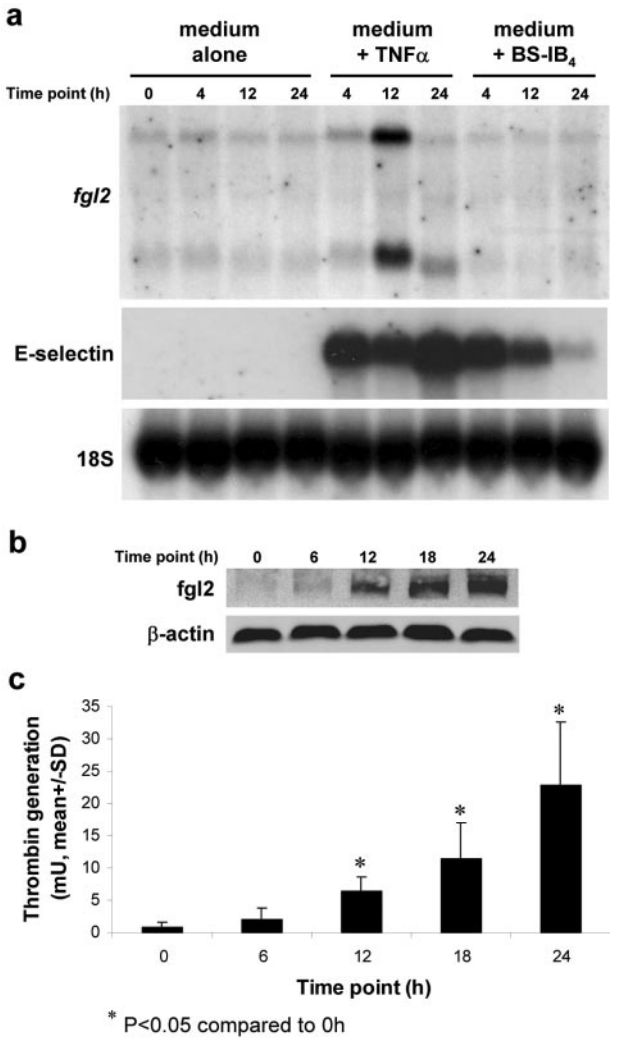

FIGURE 5. Pfgl2 expression and thrombin generation by porcine aortic endothelial cells. *a*, Representative Northern blot demonstrating induction of *pfgl2* and E-selectin mRNA by activation of PAECs with human TNF-α. Engagement of the α-gal epitope by BS-IB$_4$ induced E-selectin mRNA but not *pfgl2*. *b*, Representative Western blot demonstrating induction of pfgl2 protein expression in PAECs in response to activation with human TNF-α. *c*, Graph of thrombin generated from human prothrombin by intact PAECs activated with human TNF-α. Thrombin generation after 12, 18, and 24 h was significantly greater than at baseline ($t = 0$ h; $p < 0.05$; graph represents combined data from four separate experiments).

fgl2 within the grafts. Analysis of these grafts revealed an absence of staining in vascular ECs at baseline (Fig. 6*e*). After transplantation, cardiac xenografts demonstrated persistent induction of β-galactosidase activity in ECs beginning on POD 1, indicating transcriptional activation of *fgl2* in vascular ECs after xenotransplantation (Fig. 6*f*). In *fgl2*$^{+/-}$ grafts, endothelial induction of *fgl2* was associated with intravascular thrombosis and AVR. Low-intensity β-galactosidase staining of cardiomyocytes was apparent at

e, Medium and large-sized arteries and veins in the corticomedullary region of the kidney. Arteries show irregularity of cells in the wall, and smaller branches demonstrate luminal narrowing with fibrinoid necrosis of the wall. *f*, Immunostaining for fgl2 shows positivity in vessels in the same general area as that described in *e*. Note that the vein in the center has normal structure, whereas several arteries shown in cross-section show fibrinoid necrosis and occlusion of the lumen.

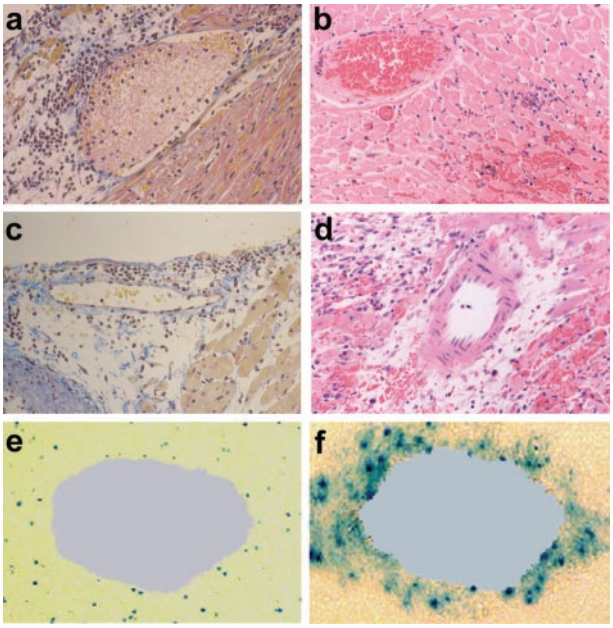

FIGURE 6. Histopathology and β-galactosidase staining of representative sections from mouse-to-rat cardiac xenografts. *a* and *b*, Sections from an *fgl2*$^{+/+}$ xenograft on POD 3 demonstrating typical features of AVR, including interstitial hemorrhage and intravascular thrombosis in a coronary vein branch in the right atrium (*a*, MSB stain) and a small artery of the ventricular myocardium (*b*, H&E). *c* and *d*, Sections from *fgl2*$^{-/-}$ xenografts on POD 3 demonstrating a coronary vein branch in the right atrium (*c*, MSB stain) and a small artery in the ventricular myocardium (*d*, H&E) with no evidence of intravascular thrombosis. *e* and *f*, β-Galactosidase staining (blue) of sections from the ventricular myocardium of *fgl2*$^{-/-}$ cardiac xenografts (single vessel lumen at center), revealing an absence of *fgl2* promoter activity in vascular endothelial cells at baseline (*e*), in contrast with the transcriptional activation of *fgl2* evident on POD 3 after xenotransplantation (*f*).

all time points, suggesting a low level of constitutive *fgl2* promoter activity in cardiomyocytes but not ECs (nuclear staining seen due to nuclear localization signal on the β-galactosidase protein; cytoplasmic staining represents ongoing protein synthesis). Negative control sections from *fgl2*$^{+/+}$ mice that lack the β-galactosidase reporter gene demonstrated no staining (not shown).

Discussion

Surmounting the barrier of AVR will require the identification and targeting of discrete pathways that contribute to fibrin deposition. In this report, we have provided evidence that these pathways include induction of fgl2 on the vascular endothelium of xenografts.

Cloning and chromosomal localization of the porcine *fgl2* gene revealed similarities to its human and murine counterparts. The single-copy *pfgl2* gene locus was identified at porcine chromosome 9q16-17. Comparative maps of chromosomal homology between species reveal that the *fgl2* gene locus is present on homologous regions of porcine chromosome 9, human chromosome 7, and mouse chromosome 5 (30–33). The successful production of gene-targeted *fgl2* knockout mice (8) suggests that the *fgl2* gene would be amenable to similar manipulation in the pig.

Like the human and mouse genes, the functional significance of two transcripts from the porcine *fgl2* gene has not been determined; however, the frequent occurrence of destabilizing nucleotide sequences (e.g., AUUUA) in the 3′ untranslated region (UTR) of the longer mRNA transcript suggests that posttranscriptional mechanisms, in combination with complex transcriptional regulation (34), ensure tightly regulated expression of fgl2 in vivo. Variability in the constitutive expression of *pfgl2* mRNA between porcine tissues is similar to patterns observed in other species (35). This pattern may reflect tissue-specific populations of cell types, such as lymphocytes or myocytes, in which constitutive fgl2 expression has been documented (36). The function of constitutively expressed fgl2 remains to be conclusively determined and is the subject of ongoing studies using fgl2-deficient mice.

Characterization of recombinant pfgl2, expressed in a baculovirus system, revealed that the protein was expressed on the cell surface, in keeping with previous observations documenting membrane-associated expression of this protein on macrophages and endothelial cells (8, 37). In contrast with the incompatibilities reported between other porcine and human coagulation proteins (16), functional assays revealed that recombinant pfgl2 protein was capable of generating active thrombin from human prothrombin. The activity of the recombinant porcine fgl2 protein was very similar to the activity of recombinant human fgl2 protein that we generated using the same baculovirus expression system (our unpublished observations). This suggests that expression of porcine fgl2 protein constitutes a mechanism for the direct production of thrombin by porcine cells and a relevant source of procoagulant activity in the pig-to-primate combination.

Immunohistochemical studies of pig-to-baboon kidney xenografts undergoing AVR revealed that pfgl2 was most intensely expressed in small vessels and glomerular capillaries, suggesting that localized generation of thrombin by fgl2 at these sites may contribute to the pathogenesis of the thrombotic microangiopathy that is a key manifestation of AVR in porcine kidney xenografts (38). Tissue infiltration by recipient macrophages and NK cells was not a prominent feature, suggesting that most of the pfgl2 protein was being produced by graft endothelial cells. Because the tissues examined in this study were harvested either from untransplanted organs or from grafts in which AVR was already occurring, further studies using protocol graft biopsies at predetermined postoperative intervals are needed to more clearly define the kinetics of pfgl2 induction in relationship to the evolution of AVR in the pig-to-baboon model.

Having identified pfgl2 expression on the endothelium of rejecting xenografts in vivo, we studied porcine endothelial cells in vitro to identify factors responsible for pfgl2 induction in these cells. Activation of vascular endothelial cells has been shown to be a key feature of xenograft AVR in vivo (39). Preliminary sequence analysis of the proximal promoter of the *pfgl2* gene revealed multiple binding sites for transactivating factors such as AP-1, suggesting that this gene would be inducible upon cellular activation. We observed that activation of PAECs by TNF-α, a cytokine that has been shown to be expressed at high levels in rejecting xenografts (10, 40), resulted in increased pfgl2 mRNA and protein levels that correlated with increasing amounts of thrombin generation. After adjustment for assay conditions, baseline thrombin generation by quiescent PAECs in our study was similar to that reported by Siegel et al. (20). This suggests that low-level constitutive expression of pfgl2 may contribute to the documented ability of PAECs to directly activate human prothrombin in vitro (20, 21). We also speculate that fgl2 may contribute to the previously described tissue factor-independent coagulation activity of porcine endothelial cells, complete neutralization of which required the addition of hirudin, a thrombin inhibitor (41). Conclusive experiments linking pfgl2 expression to thrombin generation in the porcine system, however, require neutralizing Abs against pfgl2 or fgl2-deficient porcine cells, which we are currently developing.

In the absence of suitable porcine reagents, the availability of gene-targeted *fgl2* knockout mice allowed us to directly examine

the importance of fgl2 to the pathogenesis of fibrin deposition in vivo using a well-described concordant rodent model of AVR (42), in which HAR is naturally averted due to the absence of high-titer preformed xenoantibodies. Similar to our findings in the pig-to-baboon model of AVR, *fgl2* was constitutively absent at baseline in the vascular ECs of $fgl2^{+/-}$ murine hearts, but was induced in the vascular ECs of mouse-to-rat cardiac xenografts undergoing AVR with thrombosis. This observation, in combination with our observation that α-gal-mediated activation of PAECs did not induce *pfgl2*, suggests that the mechanisms contributing to fgl2 induction in the context of AVR in vivo are independent of the interactions of preformed xenoantibodies with endothelial cells and may depend instead on the elaboration of proinflammatory cytokines such as TNF-α. This observation provides insight into possible reasons why Ab and complement depletion, which are successful in preventing HAR-associated thrombosis, do not prevent fibrin deposition during AVR.

Finally, we demonstrated that inhibition of fgl2 expression through the use of $fgl2^{-/-}$ donors, as a single intervention, protected mouse-to-rat cardiac xenografts from the thrombosis associated with AVR, despite an intact tissue factor pathway in fgl2-deficient mice, as we have documented previously (8). This observation provides new insights into the role of coagulation in AVR, supporting the hypothesis advanced by some investigators that specific targeting of coagulation pathways alone may ameliorate or prevent AVR independently of other interventions (43). In the absence of recipient immune suppression, survival of $fgl2^{-/-}$ grafts was not prolonged, and all grafts were rejected by a mechanism consistent with acute cellular rejection. The observation that maintenance cyclosporine treatment leads to indefinite survival of $fgl2^{-/-}$ grafts supports this and constitutes a component of additional studies examining precise mechanisms responsible for the rejection of these xenografts (M. Mendicino, M. Liu, A. Ghanekar, W. He, J. Turnbill, L. Fung, S. Sakamoto, P. Marsden, T. Waddell, M. J. Phillips, et al., manuscript in preparation).

In summary, this study documents the relevance of fgl2 to the thrombosis associated with AVR and suggests that this molecule may also play a role in the pathogenesis of other immunological and inflammatory conditions characterized by endothelial cell activation and intravascular fibrin deposition. Further studies involving inhibition of the porcine fgl2 through pharmacologic or genetic manipulation will be required to test the relative importance of this pathway in the discordant pig-to-primate model in vivo, in which xenoantibody, complement, and other immune mechanisms may play a more prominent role in the pathogenesis of AVR-associated thrombosis. Manipulation of fgl2, in combination with other interventions, may yield novel strategies by which to prevent AVR and extend xenograft survival.

References

1. Degen, J. L. 1999. Hemostatic factors and inflammatory disease. *Thromb. Haemostasis 82:858*.
2. Opal, S. M., and C. T. Esmon. 2003. Bench-to-bedside review: functional relationships between coagulation and the innate immune response and their respective roles in the pathogenesis of sepsis. *Crit. Care (Lond.) 7:23*.
3. Yang, Y. H., P. Carmeliet, and J. A. Hamilton. 2001. Tissue-type plasminogen activator deficiency exacerbates arthritis. *J. Immunol. 167:1047*.
4. Neale, T. J., P. G. Tipping, S. D. Carson, and S. R. Holdsworth. 1988. Participation of cell-mediated immunity in deposition of fibrin in glomerulonephritis. *Lancet 2:421*.
5. Edwards, R. L., and F. R. Rickles. 1978. Delayed hypersensitivity in man: effects of systemic anticoagulation. *Science 200:541*.
6. Chan, C. W., M. W. Chan, M. Liu, L. Fung, E. H. Cole, J. L. Leibowitz, P. A. Marsden, D. A. Clark, and G. A. Levy. 2002. Kinetic analysis of a unique direct prothrombinase, fgl2, and identification of a serine residue critical for the prothrombinase activity. *J. Immunol. 168:5170*.
7. Li, C., L. S. Fung, S. Chung, A. Crow, N. Myers-Mason, M. J. Phillips, J. L. Leibowitz, E. Cole, C. A. Ottaway, and G. Levy. 1992. Monoclonal anti-prothrombinase (3D4.3) prevents mortality from murine hepatitis virus (MHV-3) infection. *J. Exp. Med. 176:689*.
8. Marsden, P. A., Q. Ning, L. S. Fung, X. Luo, Y. Chen, M. Mendicino, A. Ghanekar, J. A. Scott, T. Miller, C. W. Chan, et al. 2003. The fgl2/fibroleukin prothrombinase contributes to immunologically mediated thrombosis in experimental and human viral hepatitis. *J. Clin. Invest. 112:58*.
9. Clark, D. A., G. Chaouat, P. C. Arck, H. W. Mittruecker, and G. A. Levy. 1998. Cytokine-dependent abortion in CBA $\times$ DBA/2 mice is mediated by the procoagulant fgl2 prothrombinase. *J. Immunol. 160:545*.
10. Bach, F. H., H. Winkler, C. Ferran, W. W. Hancock, and S. C. Robson. 1996. Delayed xenograft rejection. *Immunol. Today 17:379*.
11. Cooper, D. K., B. Gollackner, and D. H. Sachs. 2002. Will the pig solve the transplantation backlog? *Annu. Rev. Med. 53:133*.
12. Cozzi, E., and D. J. G. White. 1995. The generation of transgenic pigs as potential organ donors for humans. *Nat. Med. 1:964*.
13. Kwiatkowski, P., and R. E. Michler. 2001. Concordant cardiac xenotransplantation. *J. Card. Surg. 16:383*.
14. Bach, F. H., S. C. Robson, C. Ferran, H. Winkler, M. T. Millan, K. M. Stuhlmeier, B. Vanhove, M. L. Blakely, W. J. van der Werf, E. Hofer, R. de Martin, and W. W. Hancock. 1994. Endothelial cell activation and thromboregulation during xenograft rejection. *Immunol. Rev. 141:5*.
15. Robson, S. C., D. Candinas, W. W. Hancock, C. Wrighton, H. Winkler, and F. H. Bach. 1995. Role of endothelial cells in transplantation. *Int. Arch. Allergy Immunol. 106:305*.
16. Schulte am Esch, J., Jr., X. Rogiers, and S. C. Robson. 2001. Molecular incompatibilities in hemostasis between swine and men: impact on xenografting. *Ann. Transplant. 6:12*.
17. Patterson, C., G. A. Stouffer, N. Madamanchi, and M. S. Runge. 2001. New tricks for old dogs: nonthrombotic effects of thrombin in vessel wall biology. *Circ. Res. 88:987*.
18. Cowan, P. J., A. Aminian, H. Barlow, A. A. Brown, K. Dwyer, R. J. Filshie, N. Fisicaro, D. M. Francis, H. Gock, D. J. Goodman, et al. 2002. Protective effects of recombinant human antithrombin III in pig-to-primate renal xenotransplantation. *Am. J. Transplant. 2:520*.
19. Chen, D., K. Riesbeck, J. H. McVey, G. Kemball-Cook, E. G. D. Tuddenham, R. I. Lechler, and A. Dorling. 2001. Human thrombin and FXa mediate porcine endothelial cell activation: modulation by expression of TFPI-CD4 and hirudin-CD4 fusion proteins. *Xenotransplantation 8:258*.
20. Siegel, J. B., S. T. Grey, B. A. Lesnikoski, C. W. Kopp, M. Soares, J. Schulte am Esch, Jr., F. H. Bach, and S. C. Robson. 1997. Xenogeneic endothelial cells activate human prothrombin. *Transplantation 64:888*.
21. Jurd, K. M., R. V. Gibbs, and B. J. Hunt. 1996. Activation of human prothrombin by porcine aortic endothelial cells: a potential barrier to pig to human xenotransplantation. *Blood Coagul. Fibrinolysis 7:336*.
22. Sambrook, J., E. F. Fritsch, and T. Maniatis. 1989. *Molecular Cloning: A Laboratory Manual*, 2nd Ed. Cold Spring Harbor Laboratory, Cold Spring Harbor, NY.
23. Heng, H. H., J. Squire, and L. C. Tsui. 1992. High-resolution mapping of mammalian genes by in situ hybridization to free chromatin. *Proc. Natl. Acad. Sci. USA 89:9509*.
24. Heng, H. H., and L. C. Tsui. 1993. Modes of DAPI banding and simultaneous in situ hybridization. *Chromosoma 102:325*.
25. Lin, C. C., B. M. Biederman, H. K. Jamro, A. B. Hawthorne, and R. B. Church. 1980. Porcine (*Sus scrofa domestica*) chromosome identification and suggested nomenclature. *Can. J. Genet. Cytol. 22:103*.
26. Ghanekar, A., G. Lajoie, Y. Luo, H. Yang, J. Choi, B. Garcia, E. H. Cole, P. D. Greig, M. S. Cattral, M. J. Phillips, et al. 2002. Improvement in rejection of human decay accelerating factor transgenic pig-to-primate renal xenografts with administration of rabbit antithymocyte serum. *Transplantation 74:28*.
27. Zhong, R., Y. Luo, H. Yang, B. Garcia, A. Ghanekar, P. Luke, S. Chakrabarti, G. Lajoie, M. J. Phillips, A. G. Katopodis, et al. 2003. Improvement in human decay accelerating factor transgenic porcine kidney xenograft rejection with intravenous administration of GAS914, a polymeric form of α-gal. *Transplantation 75:10*.
28. Corry, R. J., H. J. Winn, and P. S. Russell. 1973. Primarily vascularized allografts of hearts in mice: the role of H-2D, H-2K, and non-H-2 antigens in rejection. *Transplantation 16:343*.
29. Pober, J. S. 1998. Activation and injury of endothelial cells by cytokines. *Pathol. Biol. (Paris) 46:159*.
30. Hudson, T. J., D. M. Church, S. Greenaway, H. Nguyen, A. Cook, R. G. Steen, W. J. Van Etten, A. B. Castle, M. A. Strivens, P. Trickett, et al. 2001. A radiation hybrid map of mouse genes. *Nat. Genet. 29:201*.
31. Goureau, A., M. Yerle, A. Schmitz, J. Riquet, D. Milan, P. Pinton, G. Frelat, and J. Gellin. 1996. Human and porcine correspondence of chromosome segments using bidirectional chromosome painting. *Genomics 36:252*.
32. Yuwaraj, S., J. Ding, M. Liu, P. A. Marsden, and G. A. Levy. 2001. Genomic characterization, localization, and functional expression of FGL2, the human gene encoding fibroleukin: a novel human procoagulant. *Genomics 71:330*.
33. Qureshi, S. T., S. Clermont, J. Leibowitz, L. S. Fung, G. Levy, and D. Malo. 1995. Mouse hepatitis virus-3 induced prothrombinase (Fgl2) maps to proximal chromosome 5. *Genomics 29:307*.
34. Liu, M., J. L. Leibowitz, D. A. Clark, M. Mendicino, Q. Ning, J. W. Ding, C. D'Abreo, L. Fung, P. A. Marsden, and G. A. Levy. 2003. Gene transcription of fgl2 in endothelial cells is controlled by Ets-1 and Oct-1 and requires the presence of both Sp1 and Sp3. *Eur. J. Biochem. 270:2274*.
35. Levy, G. A., M. Liu, J. Ding, S. Yuwaraj, J. Leibowitz, P. A. Marsden, Q. Ning, A. Kovalinka, and M. J. Phillips. 2000. Molecular and functional analysis of the

human prothrombinase gene (HFGL2) and its role in viral hepatitis. *Am. J. Pathol. 156:1217*.
36. Marazzi, S., S. Blum, R. Hartmann, D. Gundersen, M. Schreyer, S. Argraves, F. von Fliedner, R. Pytela, and C. Ruegg. 1998. Characterization of human fibroleukin, a fibrinogen-like protein secreted by T lymphocytes. *J. Immunol. 161:138*.
37. McGilvray, I. D., Z. Lu, A. C. Wei, A. P. Dackiw, J. C. Marshall, A. Kapus, G. Levy, and O. D. Rotstein. 1998. Murine hepatitis virus strain 3 induces the macrophage prothrombinase fgl-2 through p38 mitogen-activated protein kinase activation. *J. Biol. Chem. 273:32222*.
38. Shimizu, A., S. M. Meehan, T. Kozlowski, T. Sablinski, F. L. Ierino, D. K. C. Cooper, D. H. Sachs, and R. B. Colvin. 2000. Acute humoral xenograft rejection: destruction of the microvascular capillary endothelium in pig-to-non-human primate renal grafts. *Lab. Invest. 80:815*.
39. Holzknecht, Z. E., K. L. Kuypers, T. B. Plummer, J. Williams, M. Bustos, G. J. Gores, G. J. Brunn, and J. L. Platt. 2002. Apoptosis and cellular activation in the pathogenesis of acute vascular rejection. *Circ. Res. 91:1135*.
40. Candinas, D., S. Belliveau, N. Koyamada, T. Miyatake, P. Hechenleitner, W. Mark, F. H. Bach, and W. W. Hancock. 1996. T cell independence of macrophage and natural killer cell infiltration, cytokine production, and endothelial activation during delayed xenograft rejection. *Transplantation 62:1920*.
41. Chen, D., K. Riesbeck, G. Kemball-Cook, J. H. McVey, E. G. D. Tuddenham, R. I. Lechler, and A. Dorling. 1999. Inhibition of tissue factor-dependent and independent coagulation by cell surface expression of novel anticoagulant fusion proteins. *Transplantation 67:467*.
42. Soares, M. P., Y. Lin, J. Anrather, E. Csizmadia, K. Takigami, K. Sato, S. T. Grey, R. B. Colvin, A. M. Choi, K. D. Poss, and F. H. Bach. 1998. Expression of heme oxygenase-1 can determine cardiac xenograft survival. *Nat. Med. 4:1073*.
43. Dorling, A., and R. I. Lechler. 2001. Disordered thromboregulation after xenografting. *Curr. Opin. Organ Transplant. 6:36*.
44. BD PharMingen. 1999. *Baculovirus Expression Vector System Instruction Manual*, 6th Ed. BD PharMingen, San Diego, CA.